AN INDEPENDENT VERIFICATION OF LINAC ISOCENTER

A Thesis
Presented to
The Academic Faculty

By

Christopher Bayer

In Partial Fulfillment
of the Requirements for the Degree

Master of Science in Medical Physics

in the

George W. Woodruff School of Mechanical Engineering

Georgia Institute of Technology
August 2019

AN INDEPENDENT VERIFICATION OF LINAC ISOCENTER

Approved By:

C.-K. Chris Wang – Academic and Thesis Advisor
Professor, *Medical Physics*

Anna Erickson – Thesis Committee Member
Associate Professor, *Nuclear & Radiological Engineering*

Eric Scott Elder – Thesis Committee Member
Adjunct Associate Professor

ACKNOWLEDGEMENTS

I would like to thank Dr. Chris Wang for the idea behind the project along with his guidance and assistance with the project in its entirety. I would also like to thank Dr. Eric Elder and Beth Bradshaw Ghavidel for allowing me and assisting me in taking images on the Varian Trilogy and Varian TrueBeam at Emory University Hospital Midtown. I would like to thank Gregory Szalkowski for assisting me with taking images on Georgia Institute of Technology's Varian Clinac iX. Lastly, I would like to thank Jack Butchko and Emelody Worldwide Inc. for producing the phantom.

TABLE OF CONTENTS

LIST OF FIGURES

LIST OF TABLES

LIST OF EQUATIONS

LIST OF SYMBOLS AND ABBREVIATIONS

BB	Ball Bearing
CBCT	Cone Beam Computed Tomography
cm	Centimeter
EPID	Electronic Portal Imaging Device
IsoCal	Isocenter Calibration
kV	Kilovolt
Linac.	Linear Particle Accelerator
mm	Millimeter
MPC	Machine Performance Check
MV	Megavolt
OBI	On-Board Imaging
QA	Quality Assurance
UI	User Interface
2-D	Two-Dimensional
3-D	Three-Dimensional

I	Number of pixels above 50% penumbra value
J	Total number of images
K	Total number of ball bearings

CHAPTER 1. Introduction

Since the initial tests in the late 1950's, the linear particle accelerators (linacs) is used to treat multiple forms of cancer. Linacs have led to millions of treatments across many forms of cancer, including prostate cancer, lung cancer, breast cancer, and brain tumors, to name a few [1]. More than 50 years later, companies like Varian and Elekta continually produce advanced and high-precision linacs capable of treating more complicated tumor forms while giving greater dose sparing to the nearby healthy tissues that surround a tumor. To ensure the accuracy and precision of these powerful machines, much effort of calibration and measurement is put into commissioning them before they are approved for clinical use. A major method used to ensure the accuracy and precision of a linac system is to determine the uncertainties associated with the isocenter of the linac.

The isocenter is the theoretical point where all mechanical components of the linac, which include the gantry, couch, and collimator, rotate around, as well as the intersection point of the radiation beam at all gantry angles. If all was perfect, then the isocenter would be a point. In reality, however, the isocenter occupies a three-dimensional region rather than a theoretical point. In recent years, manufacturers have developed ways to determine this region of error. For example, the new Varian linacs (e.g. Truebeam and Edge) are equipped with the IsoCal (Isocenter Calibration) system, which includes a specialized code and manufacturer-built equipment. While Elekta utilizes its XVI clinical program, which works with a variety of phantoms [2]. Looking closer at the Varian IsoCal system, it uses a tray that sits in the head of the linac, and a phantom that is attached to the treatment couch. The IsoCal software automatically takes images of the phantom using the kilovoltage (kV) cone beam computed tomography (CBCT) system and the Megavoltage (MV) beam and electronic portal imaging device (EPID) system to calculate a variety of machine parameters, like collimator rotation tolerances, beam output deviations, and couch parameters. The parameters that will be scrutinized the most will be the centroid location and size associated with the isocenter region that the IsoCal outputs.

This thesis aims to replicate the Varian's IsoCal system, on an older Varian Clinac® iX and Varian Trilogy. Both linacs do not have the IsoCal phantom and built-in software to determine the precision of the isocenter, and currently must rely on other tests like the Winston-Lutz test for isocenter verification. Chapter 2 first gives a historical review of the various isocenter verification methods, describes the Varian's IsoCal system, and then used IsoCal system to demonstrate the method. Chapter 3 presents the isocenter verification method used in this thesis and describes the three-dimensional (3-D) phantom associated with the method. Chapter 4 presents and discusses the results obtained at the Georgia Institute of Technology's Clinac iX and the Emory University Hospital's Trilogy and TrueBeam systems. Chapter 5 provides the conclusions of the thesis.

CHAPTER 2. Background

2.1 Quality Assurance of Linear Particle Accelerators for Radiation Therapy

In 1956, Henry Kaplan was able to use a linear accelerator (linac) at Stanford to treat the eye tumor of a patient [1]. This was the first human cancer treatment using a linac-based x-ray and has paved the way for advancement of radiation treatment using linacs. Modern linacs produced by companies, like Varian and Elekta, can treat various forms of cancer all over the patient's body. With the development of clinical linacs, the problem of ensuring the accuracy of beam location with the patient's tumor site became an issue. This has led to the creation and use of concurrent on-board imaging (OBI) with linacs. Initially in the late 1950's, Cobalt-60 sources were used to take images of the patients, and the imaging system was its own independent system, separate from the linac. In 1966 the first kilovolt (kV) x-ray source was mounted in the collimator of a linac to produce a beam's eye view projection of the patient. This pursuit of treatment beam accuracy pushed the medical physics community to develop efficient ways of quality assurance (QA) for linacs. The development of Megavolt (MV) x-ray detectors helped with this and made it possible to view an image that replicates exactly what the treatment beam produces. This function is used extensively in a clinical application to line the patients up with the treatment plan before each individual treatment. The MV imager has also led to better tests to verify the accuracy of the linac as a whole.

In 1988 Lutz et. al. created a test to determine the accuracy of various radiosurgery components [3]. This is known as the Winston-Lutz test. It involves a metal marker being placed at the physical isocenter of the linac and then images of the marker are traced on radiographic films. The physical movement of the marker across the films determines the discrepancy between the beam's center as the linac's components moves around the marker. While Winston-Lutz test works well, advancements have been made to allow MV images to be processed almost instantly and software can now track multiple markers over dozens of images. These advancements formed the foundation for Varian's IsoCal system, which was developed for machine QA with the use of MV and kV images.

2.2 IsoCal System

2.2.1 IsoCal System Overview

The IsoCal system contains a manufacturer built phantom, linac head attachment, and software that allows clinicians to measure and validate a variety of machine parameters. Currently, it is usable on the Varian TrueBeam and Edge radiation therapy linacs. To develop a baseline, the Isocal system was used with the Varian TrueBeam system at Emory University Hospital Midtown location. The IsoCal system is able to calculate and validate the isocenter size and location, offset of the beam center from collimator rotation, beam output deviations, and couch parameters. This is accomplished through the use of the kV cone beam computed tomography (CBCT) imager and the MV electronic portal imaging device (EPID). For the baseline, the main focus of testing the IsoCal system was obtaining the results of the isocenter size and location from the MV beam and EPID.

2.2.2 The IsoCal Tray

The first physical piece of the system is a tray that is to be mounted to the head of the linac. As shown in Figure 1, the tray contains a six millimeter (mm) stainless steel pin, being used to test the center of the MV beam field. It is used to calibrate the accuracy of the beam center as the collimator is rotated. The collimator is moved to four 90-degree positions and images are taken for each position. The IsoCal software then tracks the center of the pin as it changes across the four images, and it can then determine the accuracy of the beam center when collimator rotation is used for clinical application [4]. The second part of the IsoCal system is a physical phantom, which is used for measuring the isocenter size and location.

Figure 1. The Varian IsoCal Tray with 6 mm steel pin.

2.2.3 The IsoCal Phantom

The IsoCal phantom is a cylindrical polyoxymethylene (Delrine) phantom. As shown in Figure 2, the phantom has a length of 24 centimeter (cm), an outside diameter of 23 cm, and an inside diameter of 20 cm, and it contains 16 tungsten ball bearings (BB's) that are 4 mm in diameter [4]. The phantom is fixed to a mount that is attached to the couch when conducting the isocenter verification, and the phantom contains five notches to align it with the room lasers; four of the notches run the length of the phantom at 90-degree intervals, and the final notch runs perpendicular to the other four at the midsection of the phantom. The phantom has a backing plate that is used to mount it to the couch, utilizing the half circle notches that run along both sides of the couch. Figure 3 shows the IsoCal phantom being mounted to the couch during an isocenter verification test.

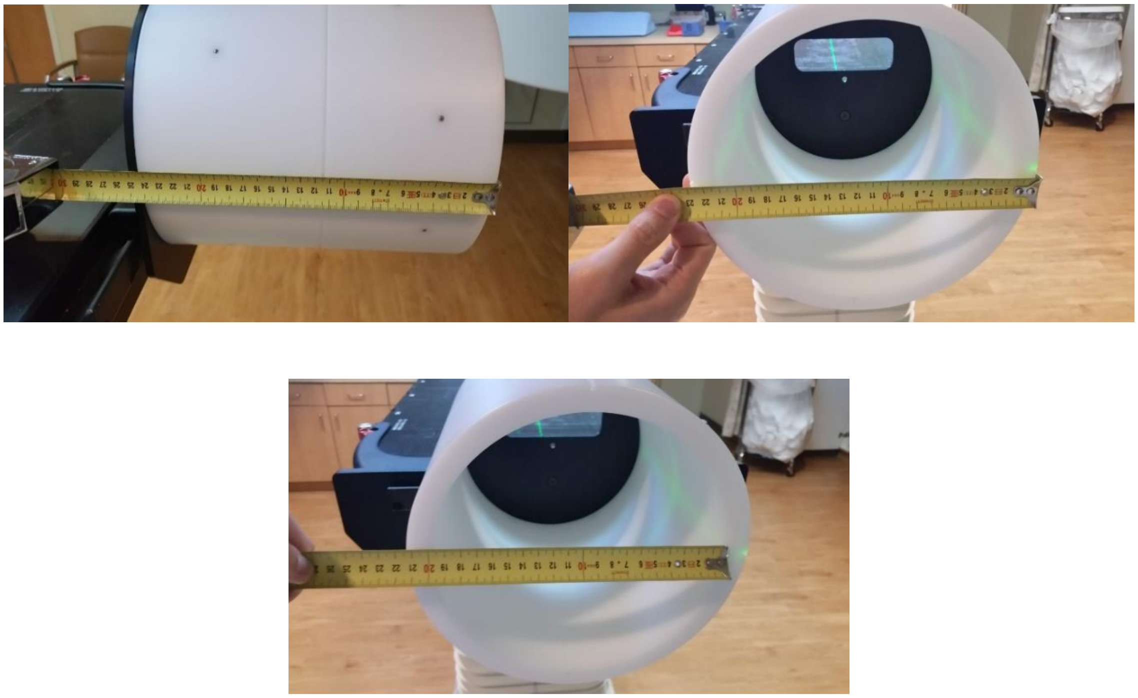

Figure 2. The Varian IsoCal phantom showing the length and inner/outer diameters.

Figure 3. The IsoCal phantom being mounted to the couch during an isocenter verification test.

2.2.4 IsoCal Setup and Procedure

The first test requires the use of the IsoCal tray, which is mounted onto the head of the linac. The test is conducted by rotating the collimator at four 90-degree intervals and taking MV images for each of the four intervals. IsoCal's software then determines the location of the steel pin at the center of the tray across the four images. Based on the steel pin locations from the four images, the program can calculate the error of the beam center from the collimator rotation.

The next test requires the use of the IsoCal phantom with both the MV imaging system and kV imaging system. The phantom is first fixed at the end of the couch and positioned at the room's isocenter using the room lasers. The operator then performs IsoCal's initial alignment check using the imagers. This initial check is to verify that the phantom is within 5 millimeters (mm) of the isocenter and will fail if it determines that this value has been exceeded. The operator will then ensure that the phantom is within the 5 mm tolerance and run the check again before the program will run fully. Once in the full IsoCal programming, the linac gantry rotates a full 360-degrees and takes 120 images throughout the entire rotation with the main beam and MV imager using a 6-MV beam. When this is complete, the couch is set at a small angle, usually less than ten degrees, and the gantry rotation process is repeated. After the MV images are completed the EPID is folded away and the CBCT-based kV imaging system is brought out to conduct the kV verification. The CBCT is used here to produce planar images, rather than its usual function of producing 3-D clinical images, replicating the two-dimensional (2-D) image format produced by the EPID of the MV imaging system. Once again, the gantry is rotated a full 360-degrees and produces 120 images using the kV imaging system. The measurement setup described above is shown in Figure 4.

All the images are then uploaded to the IsoCal software which will automatically track the ball bearing's (BB) movement and calculate the variety of machine parameters for verification. For machine verification to be accepted the parameters must be within the tolerances that Varian specifies in the program. An example of some parameters is the isocenter size calculated from the MV imager and the kV imager. The two calculated values are different but related such that both are needed to ensure the isocenter size is within the combined 0.5 mm tolerance.

Figure 4. The IsoCal phantom mounted to the end of couch for MV and kV imaging tests.

2.2.5 IsoCal Results and Comparisons

The IsoCal verification software produces a table showing all the machine parameters tested and whether the values are within the tolerances. If all the values are within tolerances, then the IsoCal verification can be accepted, otherwise the tests must be performed again. Figure 5 shows the results from the IsoCal verification performed at the Emory University Hospital's TrueBeam. It shows that the collimator rotation test produced a collimator rotation offset of 0.10^{o}, with a tolerance of $\pm 0.5^{o}$. This result is similar to a TrueBeam performance check using the IsoCal system by Allessandro Clivio et. al. who tested both the IsoCal in the Machine Performance Check (MPC) and an independent machine check to compare the differences. From the MPC and the independent machine check they found a collimator rotation offset of 0.17^{o} and 0.1^{o}, respectively.

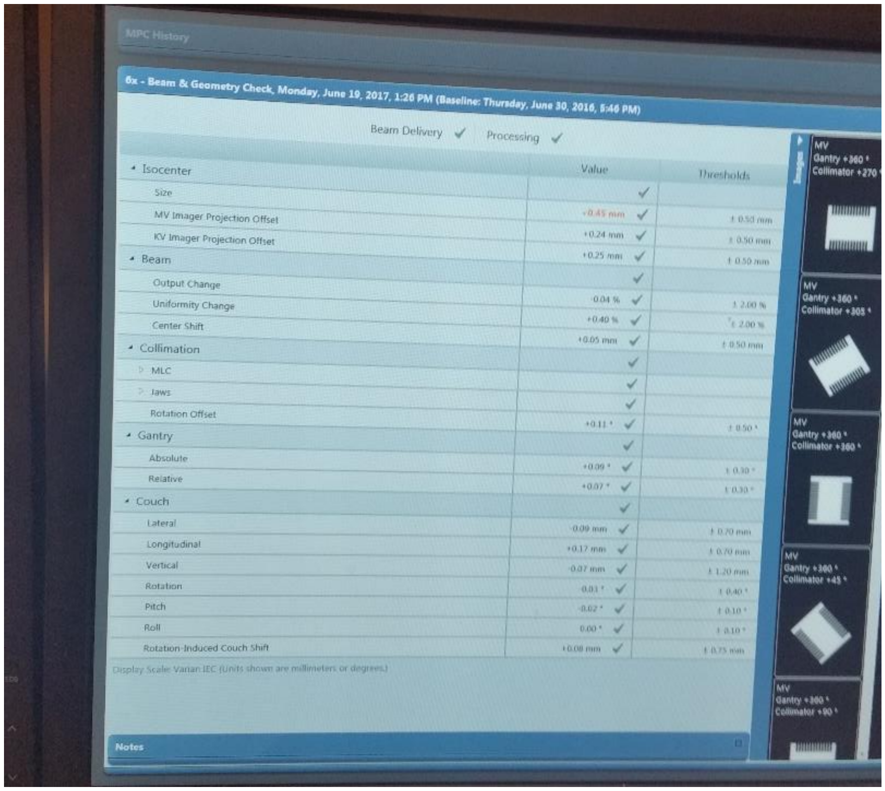

Figure 5. The machine parameter results from IsoCal verification performed at the Emory University Hospital's TrueBeam.

In the MV imager projection offset and kV imager projection offset from the Emory University Hospital's TrueBeam, the results came out to be 0.25 mm and 0.24 mm, respectively, with both values inside the ±0.5 mm tolerance. The isocenter size results came out to be 0.45 mm, which is within the ±0.5 mm tolerance for that parameter. Again, similarities are observed from Clivio et. al. tests with the IsoCal system where the MV imager projection offset came out to be 0.43 mm with the IsoCal and 0.3 mm with an independent verification. These imager projection offsets from Clivio et. al. has an error of 0.06 mm and 0.04 mm, respectively. The kV imager projection offset from Clivio et. al. came out to be 0.29 mm with the IsoCal and 0.3 mm with an independent verification. The error of the kV imager offset was found to be 0.04 mm and 0.2 mm, respectively. In the same tests the isocenter size using the IsoCal was found to be 0.42 mm and using the Winston-Lutz test was found to be 0.289 mm [5]. The above results will be compared to the results obtained from the custom-built phantom experiments (discussed in Chapter 3), which were conducted at the Georgia Institute of Technology's Varian Clinac iX and Emory University Hospital's Varian Trilogy and TrueBeam linacs.

CHAPTER 3. Methods and Design

3.1 Custom Phantom Development

The main goal was to produce a phantom that can provide similar isocenter accuracy that would cost less than Varian's IsoCal system and phantom, and have it work on any linac, new or old. The emphasis would be testing the phantom on the older linacs (e.g. the Clinac iX at Georgia Institute of Technology) since they are not equipped with the built-in Varian's IsoCal system. The phantom prototype was designed using Autodesk Inventor Professional 2016.

The phantom has a cylindrical shape, similar to the IsoCal phantom, that is 10 centimeter (cm) in outside diameter, 8.8 cm in inside diameter, and 10 cm in height. In addition, there are five grooves used to line up the center of the phantom, in similar orientation to the ones on the IsoCal phantom; where four notches run along the length of the cylinder at 90-degree intervals and one bisects the phantom perpendicular to the previous four. The phantom contains twelve cup-like openings that are used to fix the five-millimeter (mm) steel ball bearings to their respective positions, and to be able to remove the BB's for any configuration. Inside the cylinder are eight panels arranged in an octagonal pattern that can fit one-inch by one-inch square radiographic film. These panels are located directly at the midway plane of the cylinder. At the center is an opening that allows for removable attachments or radiation detection tools to be placed, an example of which would be an ion chamber. The default fitting is a cup that holds a five-millimeter BB, which can be used with the radiographic film in the eight panels to conduct a Winston-Lutz test.

The exterior BBs have the function of determining the size of the isocenter in a manner similar to the IsoCal system. The twelve BBs were chosen based on a variety of factors including prebuilt manufacturer BB counts, physical space on the custom phantom, previous studies, and error analysis. The first and foremost issue when it came to the number of BBs was the physical space the custom phantom has. The twelve BB arrangement is about the upper limit when keeping enough space between the BBs on the MV images. Weihua Mao et. al. used an $18 \times 18 \times 18$ cm^3 phantom containing thirteen BBs to track the BB movement as the gantry on a Varian Trilogy was rotated around the phantom [6]. Sun B et. al. used eleven steel plugs in a 0.5 cm water-equivalent plastic sheet to perform daily QA [7]. In addition, when a phantom containing more than twelve BBs was simulated in Autodesk Inventor, multiple BBs overlapped when rotating the beams eye view in a way the linac would produce. The number of BBs contained in the phantom also ties into the error analysis for the set of images. In the case of fewer BBs, more images would need to be taken to reduce the error propagation. With more BBs fewer images can be taken while achieving similar error propagation.

The custom phantom was fabricated using a Stratasys F370 FDM 3-D printer with the finest print quality possible of 0.005 inches, or 0.127 mm. The print took 22 hours to complete and cost was $530. Figure 9 shows the fabricated custom phantom.

Figure 6 shows the engineering drawings including the detailed dimensions of the custom phantom. Figures 7 shows the phantom with the exterior BBs fixed to positions. Figure 8 shows the phantom with center cup and BB.

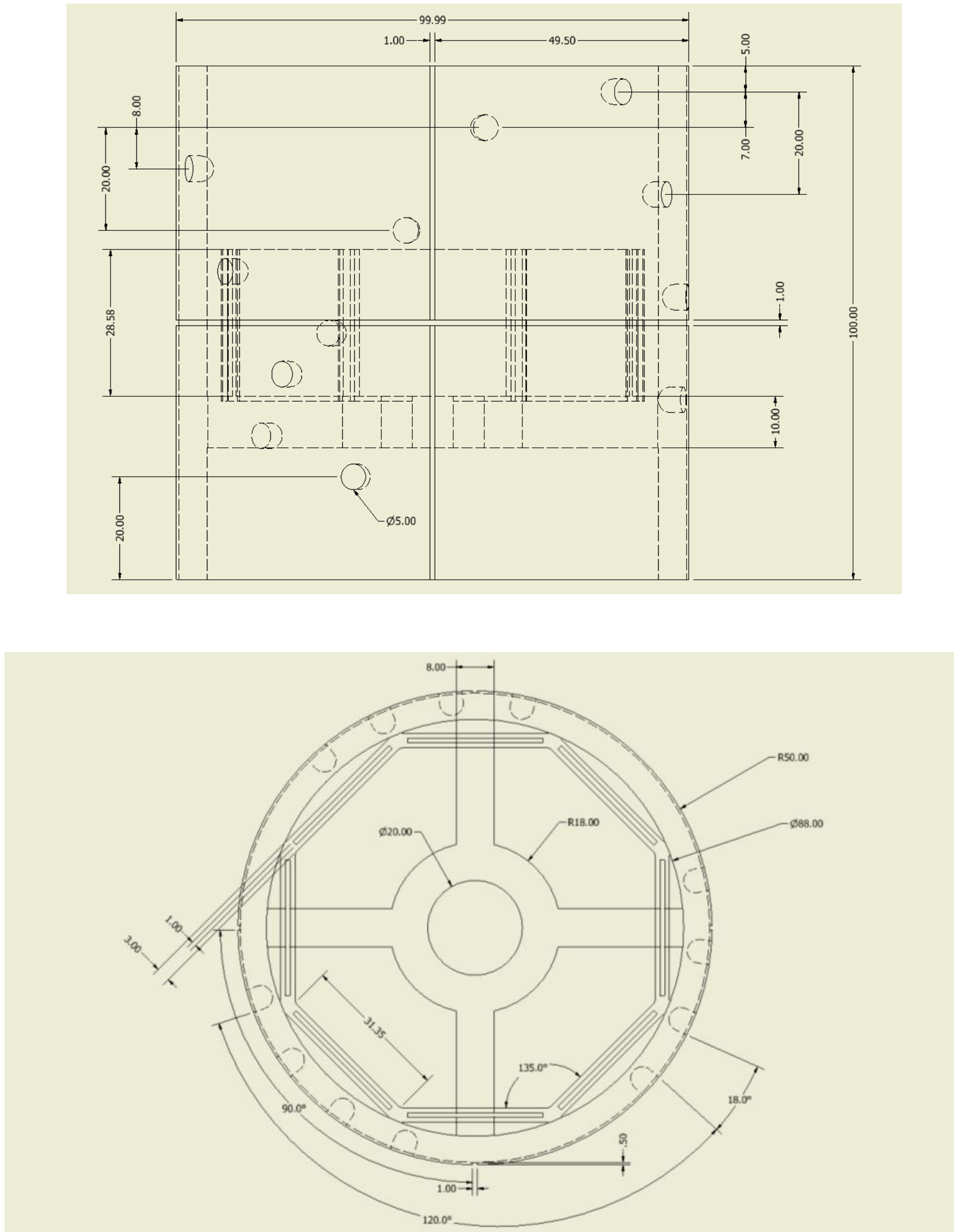

Figure 6. The engineering drawings including the detailed dimensions of the custom phantom.

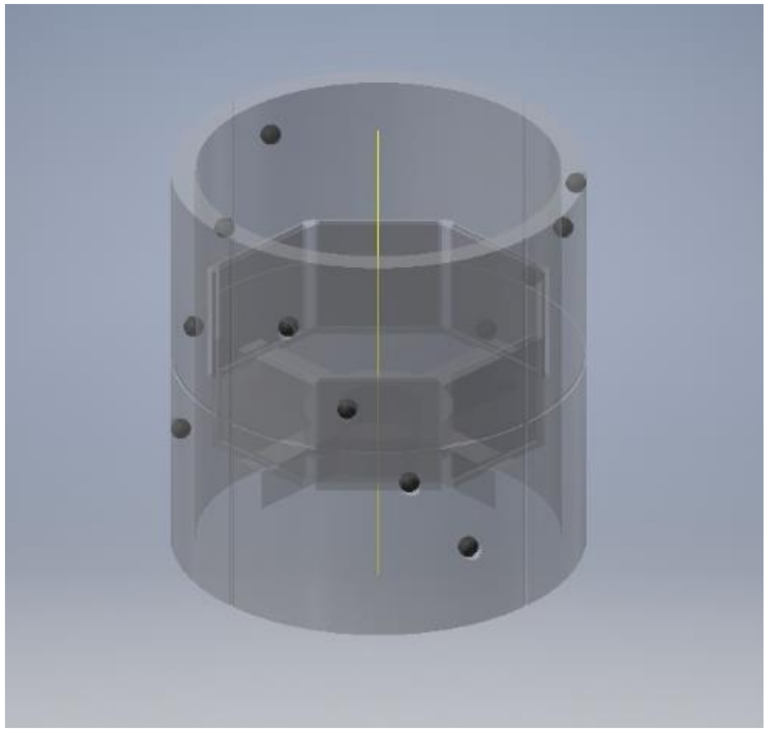

Figure 7. The phantom with the exterior BBs fixed to positions.

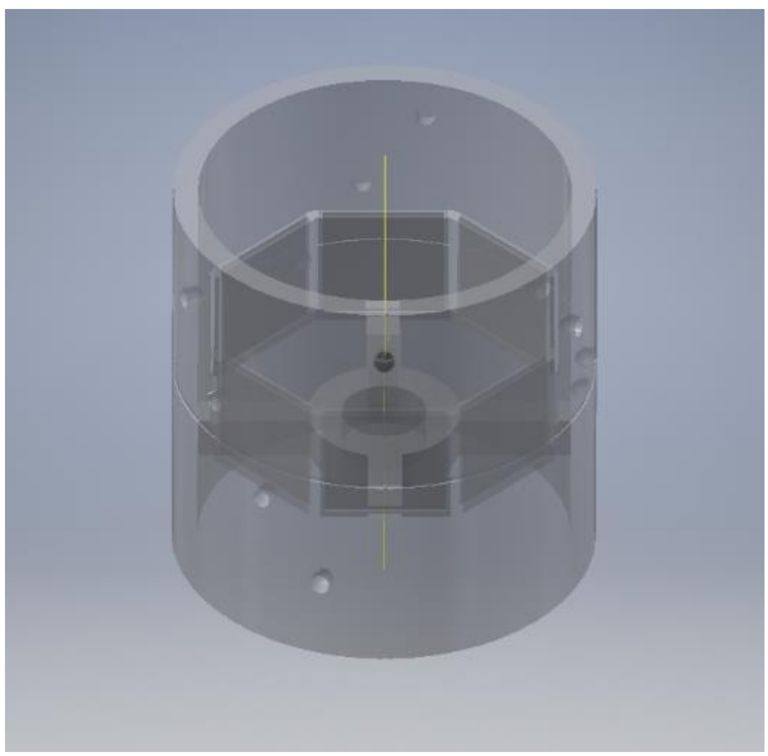

Figure 8. The phantom with the center cup and BB.

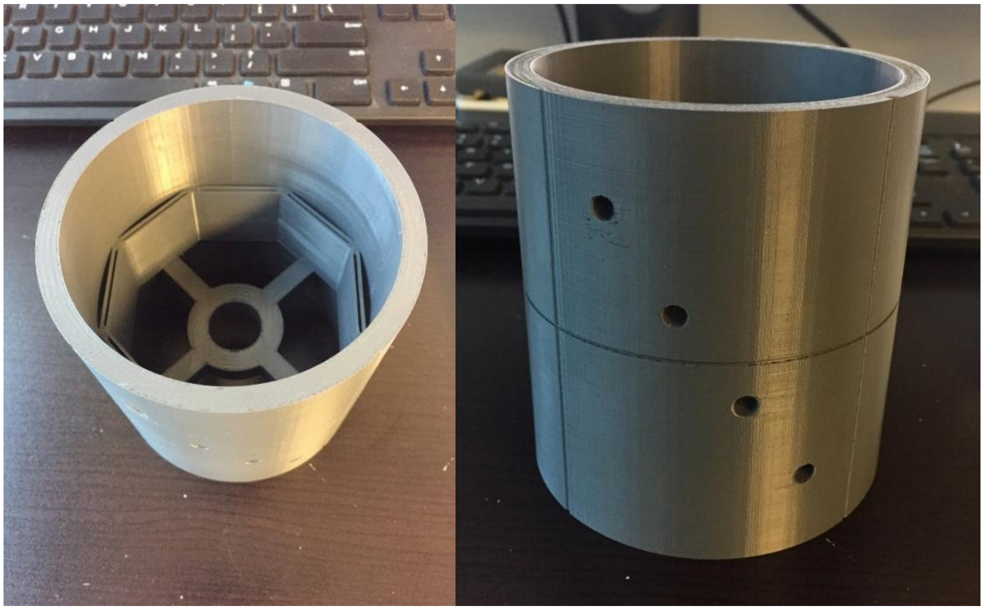

Figure 9. The fabricated custom phantom using the 3-D printing method.

3.2 Experimental Procedure

The configuration that was used in the tests was the twelve outside BBs with the middle panels absent of any film and the center cup removed. The phantom was laid out on the linac couches and aligned with the room lasers to be as close to the isocenter as possible. The software program does not require the phantom to be precisely located at the physical isocenter as it can determine the beam isocenter accurately even if the phantom is off by a few millimeters. This feature is also utilized in Varian's IsoCal system which also states the same reasoning; however, Varian clearly states that the IsoCal system must be within 5 mm of the isocenter and there are checks in place to ensure that margin is present. Currently, the custom phantom used for the tests does not have a way to mount it to the couch and thus was fastened down using adhesive tape for the tests. Figure 10 shows how the custom phantom was fastened and lined up with the room lasers at Emory University Hospital's Trilogy system.

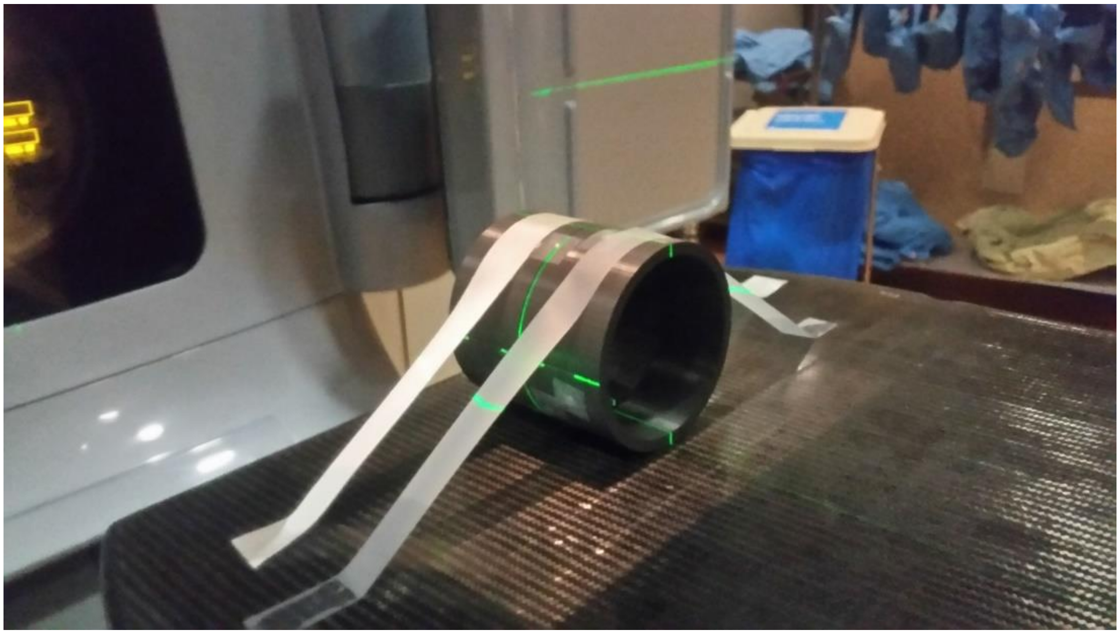

Figure 10. The custom phantom being fastened and lined up with the room lasers.

The gantry was rotated around the phantom and eight MV images were taken at 45-degree intervals to yield the 360-degree gantry rotation. This first step was done with the couch at zero degrees of angle. The next step was to angle the couch in a way so that the gantry could still move around the couch without causing a collision. On the Varian Trilogy the couch was set at a 20-degree angle. This angle allowed the head of the linac to get as close to the couch as possible without physically touching it. Figure 11 shows such a setup. On the Varian Clinac iX the couch angle was set to 15-degree to give a little more room for additional test scenarios. Again, the eight images were taken at 45-degree intervals with the couch at an angle. The last scenario, performed on the Clinac iX, was to investigate an intentional offset from the isocenter of the phantom as to how it could affect the isocenter calibration of the machine. This scenario could be encountered if room lasers are off, couch readings are incorrect, or the phantom is sloppily placed. As described above eight images were taken when the couch angle was at both zero-degree and fifteen-degree with the intentional offset.

Figure 11. Varian Trilogy experiment setup with the couch set at the 20-degree angle.

The MV images were taken through Imager Maintenance, which is in Varian's AM Maintenance program, and with the 'High Quality Images' format in the program. The program takes about four to five images while the beam is on to develop an average image that is shown in the program and saved to a dated folder. The images produced by the Clinac iX and Trilogy program are 1024 pixels wide by 768 pixels high and are saved in the DICOM format with a variety of properties including image time, imager positions, beam intensity, and couch position, to name a few. The images were then copied over to a flash drive for analysis in MATLAB. Figure 12 shows a 2-D image of the custom phantom viewed in Imager Maintenance program.

Lastly, the custom phantom was imaged on the Varian TrueBeam to develop a baseline result that could be compared to the IsoCal results and the results from the other linacs. In the TrueBeam experiment the number of images and gantry angles was kept the same as previous tests, and the images were taken while the couch was set at 0° and 15°. The TrueBeam system produced images that are 1280 pixels by 1280 pixels. Additionally, the images taken from the TrueBeam are monochrome negatives, which are shown in Figure 19, and had to be altered to monochrome positive to match the images taken from the Clinac iX and Trilogy.

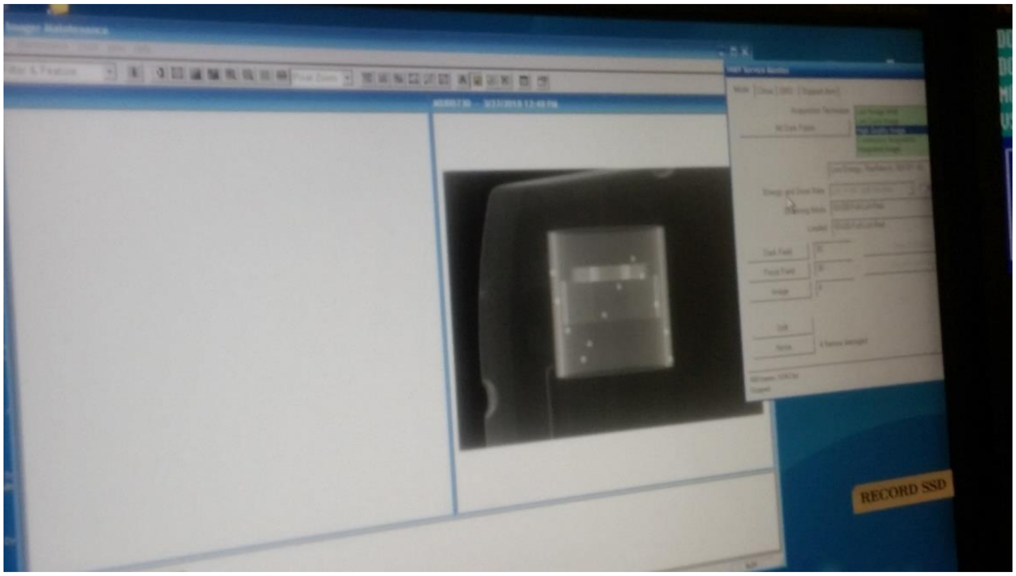

Figure 12. A 2-D image of the Custom Phantom viewed in Imager Maintenance program.

3.3 Image Analysis

A critical task of image analysis is to obtain the pixel locations of the BBs. In IsoCal the process of tracking the BB locations is automatic. However, it is noted that the software can have troubles tracking the BBs when they are present along the edge of the phantom in the image. This is the result of the greater phantom attenuation at the edges of the phantom [7]. For the custom phantom, the images were analyzed through a MATLAB program where the user manually selects the location of the BBs across all the images. An automatic BB tracking script was unsuccessful because of the additional phantom attenuation as described above. The situation is worse when the gantry angle is at 90-degrees and 270-degrees because of the additional couch attenuation occurring at the edge of the phantom. To reduce any error encountered with automatic BB tracking the BB tracking was done manually through user input in MATLAB. In this process, the user first selects the BB locations through MATLAB's 'ginput' user interface (UI) function (referred to as "box function" hereafter), which prompts a plot of thirty-pixel box overlaying where the user selected point. This selection information is passed to a function that determines pixel location corresponding to the center of the BB and the error of this calculation. This box also functions as an error for any user selections that might not fall directly in the center of the BB. To determine the center location of the BB the MATLAB program uses the 50% penumbra value between the maximum value in the box and the minimum value from the background. This 50% penumbra value is commonly used in clinical applications, especially when the beam field is blocked for treatment. This 50% value was also used by Pejman Rowshanfarzad et. al. with an isocenter experiment that used the electronic portal imaging device (EPID) to conduct a Winston-Lutz test on a Varian Trilogy linac [8].

The MATLAB program first determines the pixels whose values are greater than the 50% penumbra value. The program then uses the following equations to determine the center location of the BB.

$$\overline{x} = \frac{\sum_{i=1}^{I} (x)_i}{I} \qquad [1]$$

$$\overline{y} = \frac{\sum_{i=1}^{I} (y)_i}{I} \qquad [2]$$

where $(x)_i$ and $(y)_i$ are, respectively, the x and y coordinates of pixel i, whose value is greater than the 50% penumbra value; and I is the number of pixels whose values are greater than the 50% penumbra value. In other words, the center location coordinates $[\overline{x}, \overline{y}]$ for each BB are calculated by taking the average of the coordinate values of the pixels (within a single BB selection site) whose values lie above

50% penumbra value. Figure 13 is an image of the custom phantom from the Varian TruBeam showing a BB's center pixel location calculated by the MATLAB program.

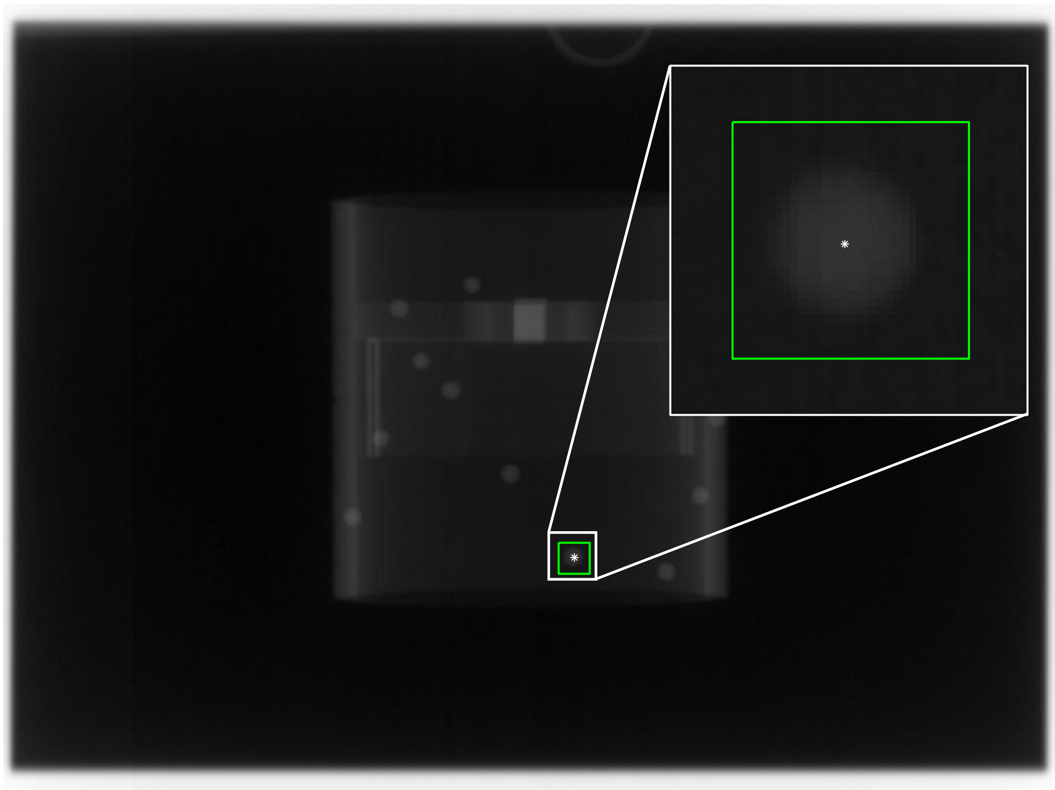

Figure 13. An image of the custom phantom from the Varian TruBeam showing a BB's center pixel location calculated by the MATLAB program.

The user selection for all BBs in a single image is shown in Figures 14 and 15. These show the BB selection process for images from the Varian Trilogy with the two images corresponding to the couch angles of zero-degree and the 20-degree, respectively. Additionally, the two images from the Clinac iX where the phantom was intentionally offset are shown in Figures 16 and 17 corresponding to the couch angles of zero-degree and 15-degree, respectively.

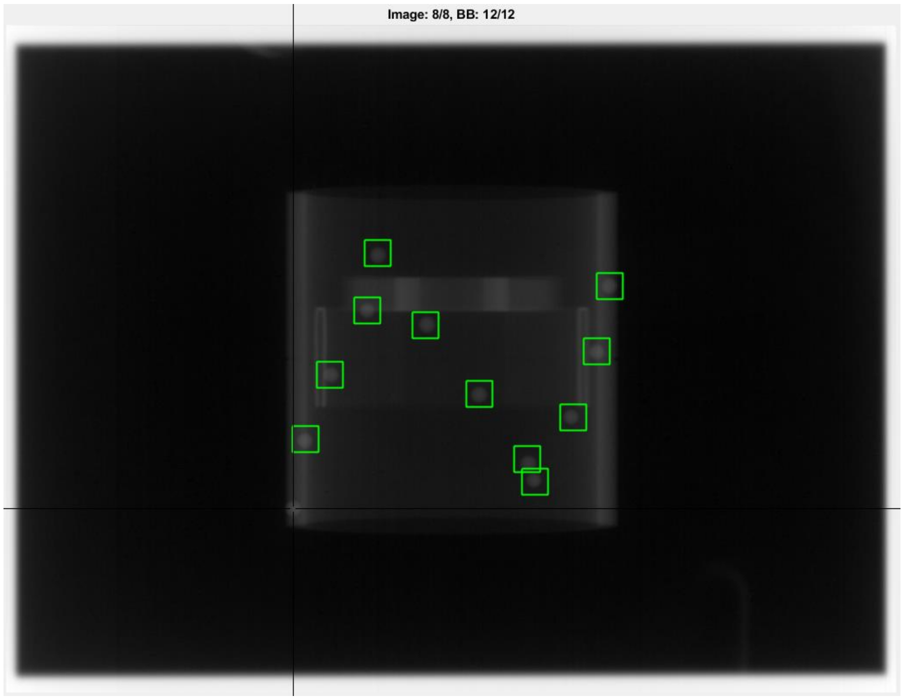

Figure 14. A Varian Trilogy image obtained with the couch angle at 0°.

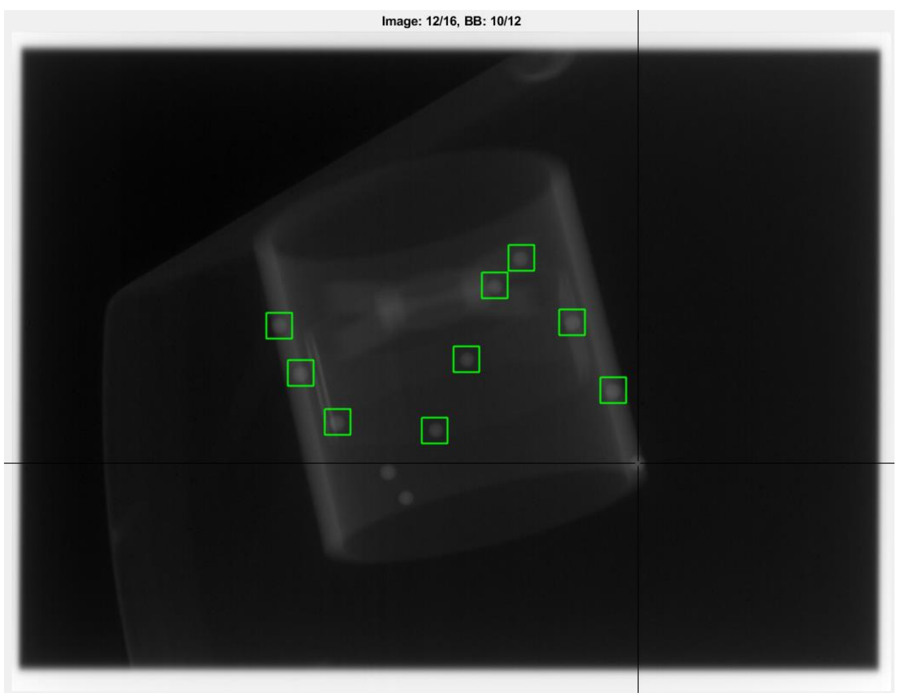

Figure 15. A Varian Trilogy image obtained with the couch angle at 20°.

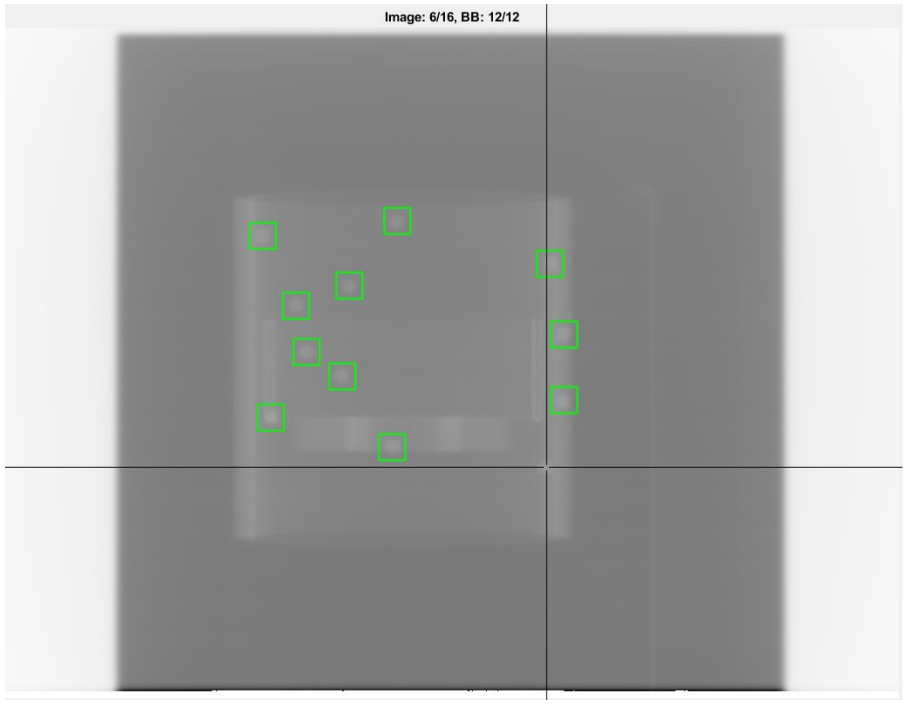

Figure 16. A Varian Clinac iX image with 2 cm offset obtained with the couch angle at 0°.

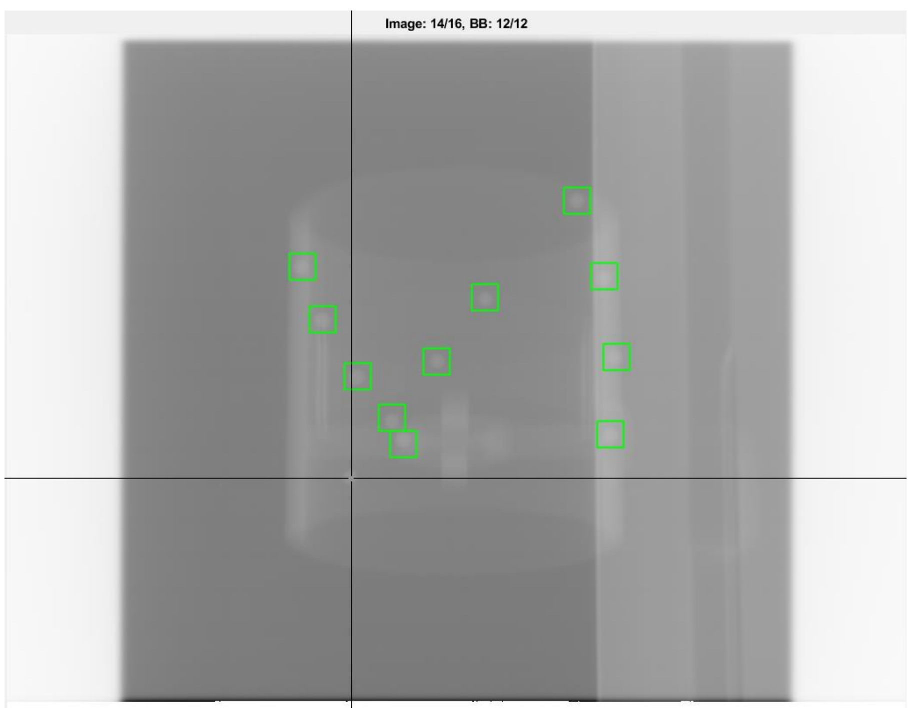

Figure 17. A Varian Clinac iX image with 2 cm offset obtained with the couch angle at 15°.

As shown in the above four figures, the user selects the BB locations using the crosshairs in MATLAB. The top of the figure keeps track of the image currently shown and the number of BBs selected. As shown in Figures 16 and 17, the images obtained from the Clinac iX are noticeably lighter than the images obtained from the Trilogy. This contrast difference will affect the error calculations for the Clinac iX analysis.

Once the user selects all BB locations on a single image across all the images from the selected gantry angles, the MATLAB program can develop a path that a BB takes and determine the rotation point for each BB. Figure 18 shows the path a BB takes after the user has completed the BB location selection process:

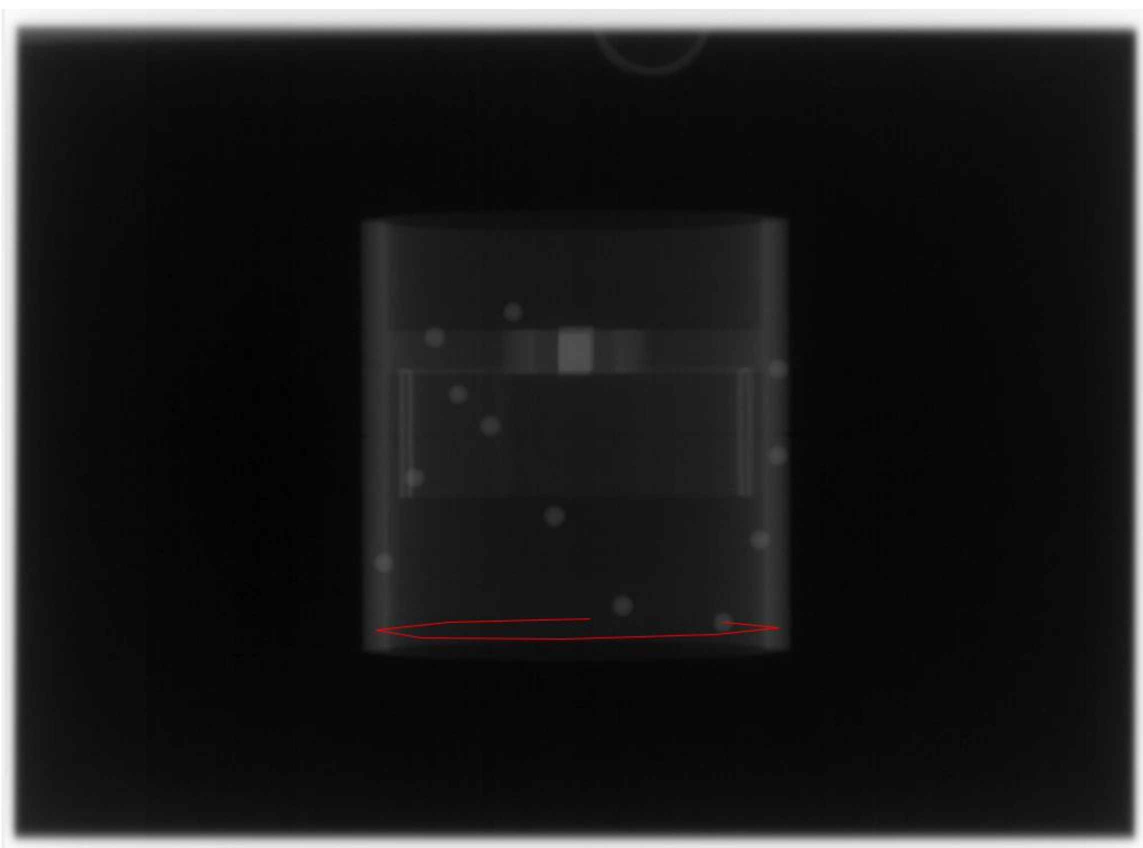

Figure 18. Path of single BB from Varian Trilogy at 0^{o} couch angle.

The x- and y-coordinates of the rotation point for each BB is calculated as:

$$x_{rot} = \frac{\sum_{j=1}^{J} (\bar{x})_j}{J} \quad [3]$$

$$y_{rot} = \frac{\sum_{j=1}^{J} (\bar{y})_j}{J} \quad [4]$$

where $(\bar{x})_j$ and $(\bar{y})_j$ are, respectively, the x and y coordinates of the BB in image j; and J is the total number of images.

The above equation tracks the location of a single BB across all the images and uses the average position to determine the rotation point for the BB. This process is done for all the BBs simultaneously across all the images as the user completes the selection process. To evaluate the errors associated with the BB locations, the MATLAB program also calculates the standard deviation for each BB location using the following equation:

$$\sigma_x = \sqrt{\frac{\sum_{i=1}^{I} (x_i - \bar{x})^2}{I}} \quad [5]$$

$$\sigma_y = \sqrt{\frac{\sum_{i=1}^{I} (y_i - \bar{y})^2}{I}} \quad [6]$$

where I is the same as that in Equations [1] and [2]. These errors are then averaged to achieve the overall error for the tracking of a single BB. This is done through the following equations:

$$\sigma_{x_{rot}} = \frac{\sum_{j=1}^{J} (\sigma_x)_j}{J} \quad [7]$$

$$\sigma_{y_{rot}} = \frac{\sum_{j=1}^{J} \left(\sigma_y\right)_j}{J} \quad [8]$$

where J is the same as that in Equations [3] and [4].

Lastly, the MATLAB program calculates the average rotation point over all 12 BBs as well as the associated errors using the following equations:

$$\bar{x}_{rot} = \frac{\sum_{k=1}^{K} \left(x_{rot}\right)_k}{K} \quad [9]$$

$$\bar{y}_{rot} = \frac{\sum_{k=1}^{K} \left(y_{rot}\right)_k}{K} \quad [10]$$

$$\sigma_{\bar{x}_{rot}} = \sqrt{\frac{\sum_{k=1}^{K} \left[\left(x_{rot}\right)_k - \bar{x}_{rot}\right]^2}{K}} \quad [11]$$

$$\sigma_{\bar{y}_{rot}} = \sqrt{\frac{\sum_{k=1}^{K} \left[\left(y_{rot}\right)_k - \bar{y}_{rot}\right]^2}{K}} \quad [12]$$

where K is the total number of BBs, which is 12 for this study.

This whole process was done with the TruBeam linac images with one additional step. In the TrueBeam image gathering, the pixel values representing the images are monochrome negatives of those representing the images produced by the Trilogy and Clinac iX linacs. Accordingly, the pixel values representing the TruBeam images were reverted to be consistent with the Trilogy and Clinac iX images. This process is shown in Figure 19.

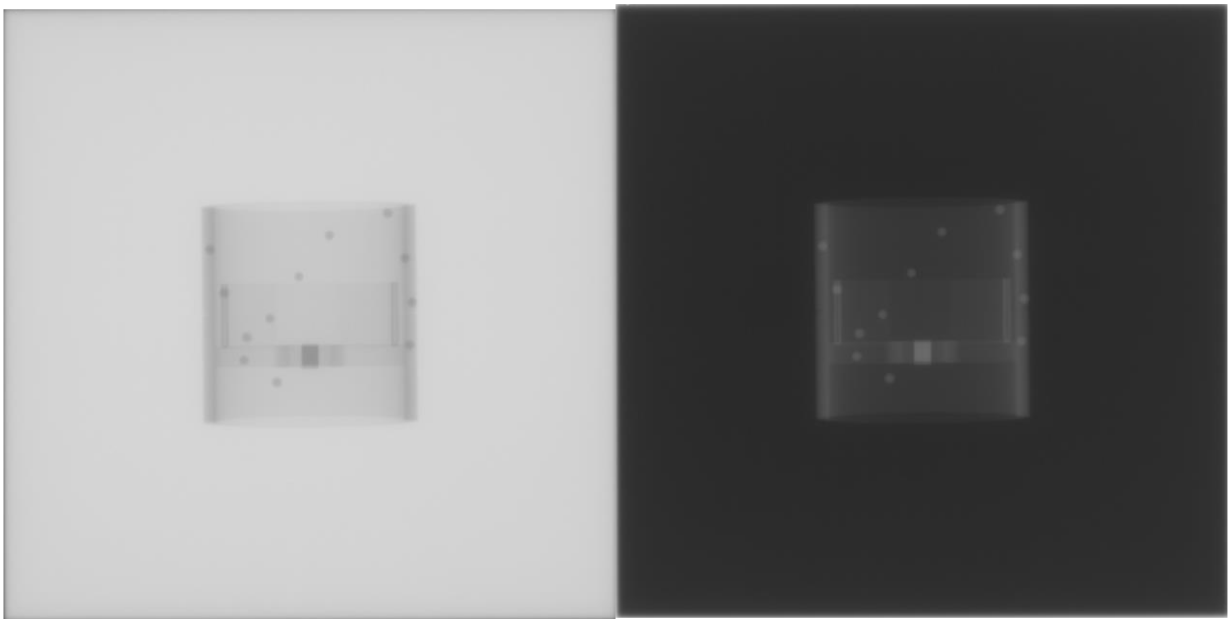

(a) (b)

Figure 19. The image from TruBeam was reverted to be consistent with the Trilogy and Clinac iX images: (a) before reversion, and (b) after reversion.

The MATLAB program is provided in Appendix A. The data gathered from the images and processed by the MATLAB program can then be used for analysis and verification of the isocenter.

CHAPTER 4. Results and Discussion

4.1 Results

The MV images of the custom phantom for the various linacs were processed by the MATLAB program, and the results were converted into Microsoft Excel tables. The full tables of the data are provided in Appendix B. The values of the average BB location, (x_{rot}, y_{rot}), were calculated from Equations 3 and 4. The corresponding errors were calculated from Equations 7 and 8. The format of the tables shows the rotational axis with their respective standard deviation. Since the MV images for Varian Trilogy and Clinac iX are made of 1024 x 768 pixels, the column pixels are denoted as 0 to 1024, and the row pixels are denoted as 0 to 768. The Varian TrueBeam images are 1280 pixels x 1280 pixels. Accordingly, the column pixels and the row pixels are both denoted as 0 to 1280. The pixel size of 0.392 × 0.392 mm^2 was used in the MATLAB program to convert the MATLAB tracking data and to determine the physical size of the isocenter.

Tables 1-8 include the important features extracted from Appendix B. In the odd-number tables, $(x_{rot})_{\max}$ and $(x_{rot})_{\min}$ are the highest and lowest pixel locations across the 12 BBs in the phantom. In the even number tables, the average pixel location across the 12 BBs, $\overline{x}_{rot}$, and the standard deviation, $\sigma_{\overline{x}_{rot}}$, were calculated from Equations 9 through 12. Lastly, $\left|(x_{rot})_{\max} - (x_{rot})_{\min}\right|$ is used to determine the size of the isocenter in the x-direction.

Tables 1, 2 – Varian Trilogy results based on 50% penumbra value.

Varian Trilogy Condensed 50% Penumbra Data		$\left(x_{rot} \pm \sigma_{x_{rot}}\right)_{max}$	$\left(x_{rot} \pm \sigma_{x_{rot}}\right)_{min}$	$\lvert(x_{rot})_{max} - (x_{rot})_{min}\rvert$	Physical Size (mm)
Couch Angle (Degrees)	0	511.333 ± 1.085	510.458 ± 1.024	0.874	0.343
	20	511.040 ± 0.886	510.279 ± 0.937	0.761	0.298
	Δ	0.293 ± 0.200	0.179 ± 0.087	0.113	0.044
	Size Difference (mm)	0.115 ± 0.078	0.070 ± 0.034	0.044	0.017

Varian Trilogy Condensed 50% Penumbra Data		$\left(\bar{x}_{rot} \pm \sigma_{\bar{x}_{rot}}\right)$	$\left(\bar{y}_{rot} \pm \sigma_{\bar{y}_{rot}}\right)$
Couch Angle (Degrees)	0	510.856 ± 0.316	413.149 ± 1.811
	20	510.758 ± 0.216	411.361 ± 1.846
	Δ	0.098 ± 0.100	1.787 ± 0.035
	Size Difference (mm)	0.038 ± 0.100	0.701 ± 0.014

Tables 3, 4 – Varian Clinac iX results based on 50% penumbra value.

Varian Clinac iX Condensed 50% Penumbra Data		$\left(x_{rot} \pm \sigma_{x_{rot}}\right)_{max}$	$\left(x_{rot} \pm \sigma_{x_{rot}}\right)_{min}$	$\lvert(x_{rot})_{max} - (x_{rot})_{min}\rvert$	Physical Size (mm)
Couch Angle (Degrees)	0	512.337 ± 0.940	511.153 ± 1.391	1.184	0.464
	15	512.354 ± 1.334	511.078 ± 0.954	1.277	0.500
	Δ	0.017 ± 0.394	0.076 ± 0.437	0.093	0.036
	Size Difference (mm)	0.007 ± 0.155	0.030 ± 0.171	0.036	0.014

Varian Clinac iX Condensed 50% Penumbra Data		$(\bar{x}_{rot} \pm \sigma_{\bar{x}_{rot}})$	$(\bar{y}_{rot} \pm \sigma_{\bar{y}_{rot}})$
Couch Angle (Degrees)	0	511.721 ± 0.373	361.499 ± 1.886
	15	511.698 ± 0.373	363.967 ± 1.876
	Δ	0.022 ± 0.001	2.468 ± 0.010
	Size Difference (mm)	0.009 ± 0.000	0.967 ± 0.004

Table 5, 6 – Varian Clinac iX data with 2 cm offset based on 50% penumbra value.

Varian Clinac iX with 2 cm Offset Condensed 50% Penumbra Data		$(x_{rot} \pm \sigma_{x_{rot}})_{max}$	$(x_{rot} \pm \sigma_{x_{rot}})_{min}$	$\lvert(x_{rot})_{max} - (x_{rot})_{min}\rvert$	Physical Size (mm)
Couch Angle (Degrees)	0	512.374 ± 1.034	511.120 ± 1.384	1.254	0.492
	15	511.990 ± 1.526	510.727 ± 0.700	1.262	0.495
	Δ	0.384 ± 0.491	0.393 ± 0.684	0.008	0.003
	Size Difference (mm)	0.151 ± 0.193	0.154 ± 0.268	0.003	0.001

Varian Clinac iX 2 cm Offset Condensed 50% Penumbra Data		$(\bar{x}_{rot} \pm \sigma_{\bar{x}_{rot}})$	$(\bar{y}_{rot} \pm \sigma_{\bar{y}_{rot}})$
Couch Angle (Degrees)	0	511.785 ± 0.387	361.602 ± 1.898
	15	511.553 ± 0.336	383.113 ± 1.866
	Δ	0.232 ± 0.051	21.511 ± 0.033
	Size Difference (mm)	0.091 ± 0.020	8.432 ± 0.013

Table 7, 8 – Varian TrueBeam data based on 50% penumbra value.

Varian TrueBeam Condensed 50% Penumbra Data		$(x_{rot} \pm \sigma_{x_{rot}})_{max}$	$(x_{rot} \pm \sigma_{x_{rot}})_{min}$	$\lvert(x_{rot})_{max} - (x_{rot})_{min}\rvert$	**Physical Size (mm)**
Couch Angle (Degrees)	0	641.373 ± 0.946	640.035 ± 0.902	1.338	0.524
	15	641.145 ± 0.884	639.940 ± 0.814	1.205	0.472
	Δ	0.227 ± 0.062	0.095 ± 0.087	0.133	0.052
	Size Difference (mm)	0.089 ± 0.024	0.037 ± 0.034	0.052	0.020

Varian TrueBeam Condensed 50% Penumbra Data		$(\overline{x}_{rot} \pm \sigma_{\overline{x}_{rot}})$	$(\overline{y}_{rot} \pm \sigma_{\overline{y}_{rot}})$
Couch Angle (Degrees)	0	640.703 ± 0.440	604.687 ± 1.546
	15	640.735 ± 0.353	605.817 ± 1.541
	Δ	0.032 ± 0.087	1.130 ± 0.006
	Size Difference (mm)	0.013 ± 0.034	0.443 ± 0.002

4.2 Analysis and Discussion

4.2.1 Data and Error Analysis

Overall the data above shows promising results of the validity of the custom phantom. When the baseline TrueBeam data is presented it is shown that the isocenter size came out to be 0.524 mm when using the 50% penumbra value, which is about 0.07 mm larger than the results using the IsoCal phantom and software. This difference comes out to be about 15% between the IsoCal results and the custom phantom results. This error may have been introduced from the image correction done in MATLAB. While the error difference is not ideal, the small difference between the isocenter's physical size is small enough to consider the results acceptable. This isocenter size verification can validate the data calculated in the Trilogy and Clinac iX tests.

When looking at the Trilogy results the 50% penumbra results gave a maximum isocenter size average of 0.321 mm. This size is considerably smaller than that of the TrueBeam results. It may have come down to the variation of the image acquisition at the time that yielded better results. With the Trilogy images they had the highest contrast out of all of them, and they did not have to be altered in any way. Subsequent runs would determine if this value is in line as to how the machine performs on a daily basis, or if the value was an anomaly.

With the Clinac iX data, it is found that the maximum isocenter size average is 0.482 mm. This value is closer to the isocenter value from the IsoCal test both with the Emory machine and the value calculated by Clivio et. al. One explanation that this value is higher than the value calculated with the Trilogy could be that the Clinac iX is not a machine used for clinical applications. Thus, the machine does not face heavy scrutiny for remaining as accurate as possible for treatments. Additionally, it is the oldest machine of the three. The manufacturing technologies have greatly improved with the Trilogy and the TrueBeam, and the physical wear is far greater in the Clinac iX from longer use. Another source that could explain the increases in size and error could come from the image quality achieved from the Clinac iX. As shown in previous images the contrast between the background and the BB's is much less and can yield higher error and a less accurate isocenter calculation.

The additionally test on the Clinac iX intentionally set the phantom 2 centimeters (cm) off from isocenter to see how the results would change. Based on the 50% penumbra result without the offset, the isocenter size with the offset did not make much of a difference. The average maximum isocenter size came out to be 0.494 mm. It is slightly higher, but within the 0.5 mm tolerance for verification. This shows that the alignment of the phantom has little effect on the results based on how the program calculates the BB movement.

Lastly, an 80% penumbra calculation was conducted through the MATLAB program. This was an effort to eliminate more error from attenuation and in sense increase the contrast of the BB's. Unfortunately, this technique did not provide the intended results. In fact, the rotational point calculations were much farther apart, and the error associated with the calculations was much higher. This yielded data that was not useful when compared to the 50% penumbra results.

4.2.2 The Custom Phantom

The custom phantom completed its intended goal of providing a cheaper system for isocenter verification that would function in a similar way to IsoCal's system. At a cost of $530 for the custom phantom it is much less expensive than the IsoCal phantom and functions in a similar manner. Since the phantom is not tied to any linac system or manufacturer it can be used on any linac with an MV or kV imager. This versatility would allow one phantom to be used for isocenter verification on multiple linacs in a small clinical setting.

The phantom does have some drawback to it. First, currently it does not have a method of mounting securing to a linac couch. This would take some mechanical investigations to devise a system that would keep the versatility and securely fasted the phantom. Another drawback discovered in the image analysis came with the relative closeness of the ball bearings (BB). While designed to be as far apart from one another as possible, when the couch was angled, and images were taken, that spread distance shrunk to smaller distances that did lead to some overlap. This could be fixed with a larger, more expensive phantom, which contradicts some of the goals with the project. Another way would be removing a few of the twelve BBs from the phantom, but more images would need to be taken to account for the increased error. And the last fix could be decreasing the couch angle, which would allow elimination of any BB overlap across the images. This overlap of the BBs is investigated and explained further below.

Another issue with the BB location on the phantom was the asymmetry of their locations. When looking at the engineering drawings the BBs are not symmetrical between the top half and bottom half on the phantom. This causes the midline between all the BBs to be different from the physical midline. While this can be overcome in the calculations, it would make the isocenter accuracy better if the BB midline was in line with the radiation isocenter in the images.

4.2.3 The MATLAB Code

While the MATLAB code performed the function needed, it was far from perfect. Manually selecting the BBs for tracking was tedious and increased the time it took to get the results. Further advancement in the code might be able to yield a better automatic tracking system in the future. This does come with a caveat that was discovered when combing through the images. The BBs take a highly elliptical path across the images as the imager moves around the phantom. This position change is from the relative distance between the BB and the imager and is exaggerated at the top and bottom of the phantom. The following image shows the path for a single BB:

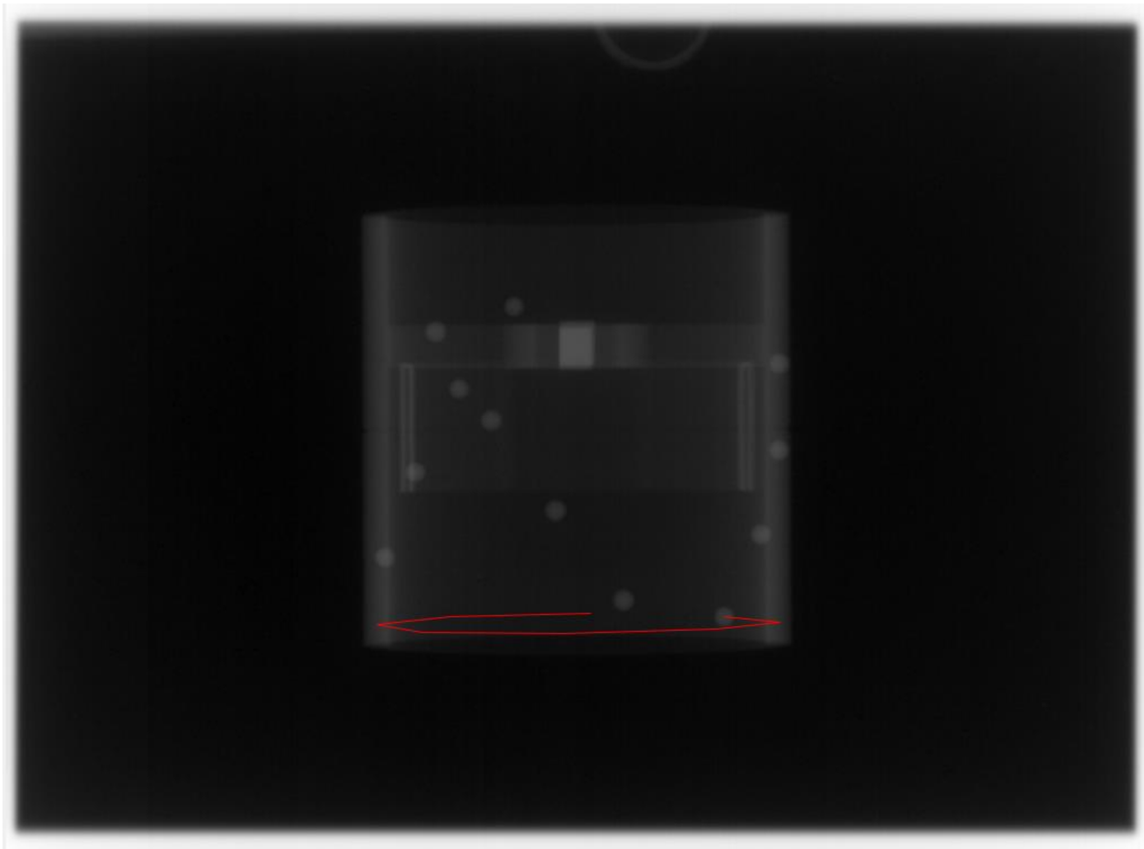

Figure 20. Path of single BB from Varian Trilogy at 0^{o} couch angle.

As seen above, the BB path is differentiated enough from the adjacent BB that they will not cross when selecting the BBs between images. This is not the case when the BBs were tracked at the high couch angles. The following images shows the path for two BBs on the Varian Trilogy at the specified couch angle:

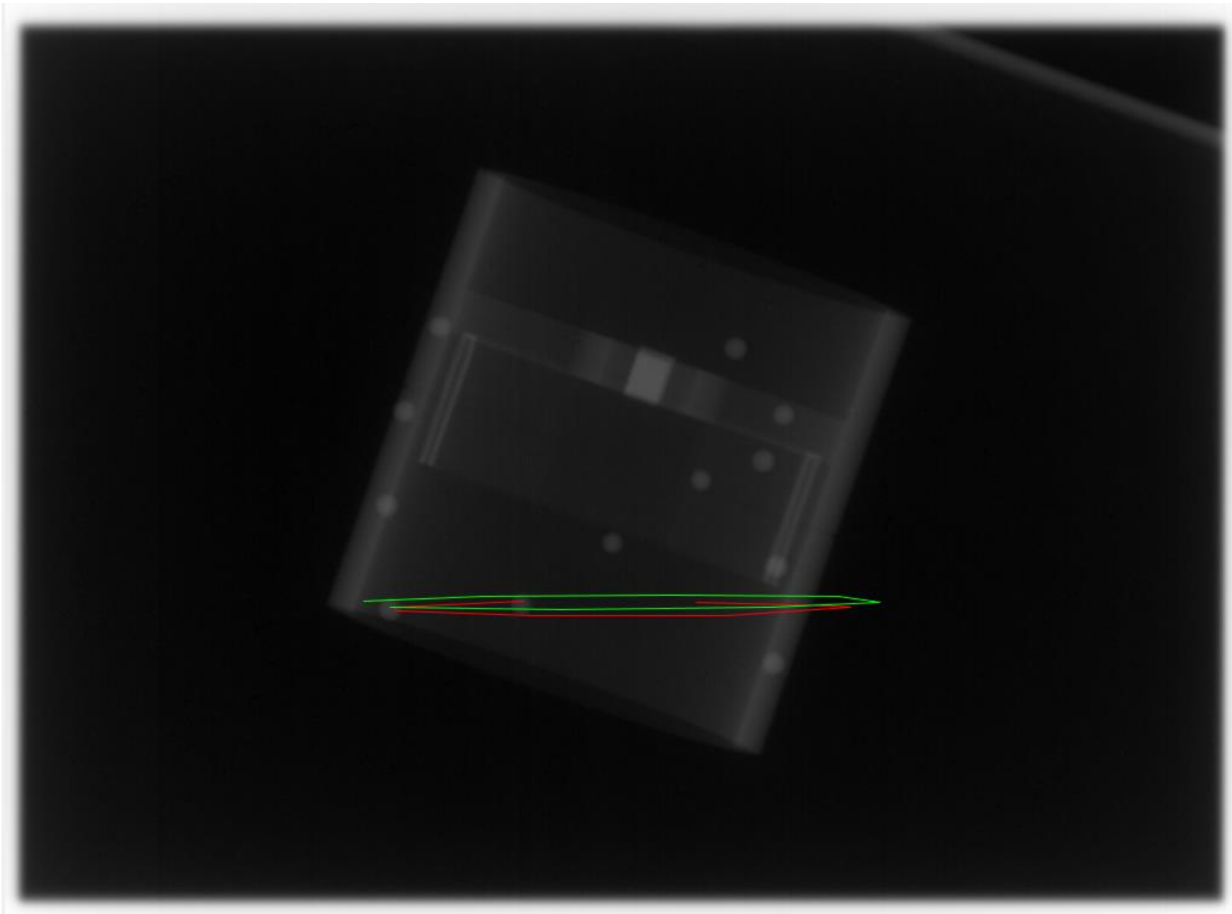

Figure 21. Paths of two BBs from Varian Trilogy at 20^{0} couch angle.

As described before the paths cross between the two BBs because of the high couch angle. This led to many issues when tracking the BBs, both in the attempt to automatically track them, and even when manually tracking them. There are a few approaches to fixing this issue, some of which are mentioned previously. This includes taking a few of the BBs out of the phantom so the distance between each BB is increased even greater. Another fix would be decreasing the couch angle to one not so high so that the row change is not as drastic. Some fixes that could be done with the program would be an estimation function that can assist the user in determining where BBs will lie when manually selecting them. Without a function of the sort the BBs had to be tracked as they visually moved between images. On a positive note, this MATLAB code was able to function identically and produce similar results whether the couch was angled, or the phantom was intentionally offset from the isocenter. The reason for this is the way the program tracks the BB's path over the images. As it is represented in the two figures above, the BB path is elliptical and centered over the middle of the imager in the column pixel direction, or width of the image. When the couch is angled or moved off center an individual BB will have its position relative to the midline altered slightly. As the gantry rotates around the phantom, this apparent position change will be mirrored on both sides of the midline. With the net result of the path still yielding the midline of the image, or in the case of the physical space, a rotation axis. Again, this is proven to be true when the phantom is intentionally offset 2 cm on the Clinac iX. The rotation axis is found to still be in the middle of the image, exactly where it is in the other experiments. The downside to this intentional offset is the BB moves a greater distance between images and increases the error in the calculations, as seen in the tables above.

While the custom program seems very robust, it is very dependent on how well the procedure was executed. It does raise a question as to how Varians' IsoCal software processes this BB path. One could deduce that this elliptical BB path occurs during the IsoCal verification, but it is unknown as to how the software handles it. It can also be concluded that the elliptical effect would be greater with the IsoCal phantom since it is a much larger phantom and the difference in distances between the BB and the imager will be much greater. Unfortunately, looking into the code is likely not possible so another aspect needs to be investigated to come to a sound conclusion in the custom phantom. This leads to a comparison of the procedures used to perform IsoCal verification and the procedure used on the custom phantom.

4.2.4 Experimental Procedure

While the experimental procedure was reenacted in a similar manner to the way IsoCal verification is conducted, there is one key factor that likely makes a large difference in results. This difference is the number of images. While the number of BBs did indeed help keep error lower in the custom phantom calculations, the low number of images taken with the custom phantom kept the error higher than the error observed in IsoCal. In IsoCal there are 120 images taken over the 360-degree rotation; in other words, one image is taken every 3 degrees of gantry rotation. In the experiments with the custom phantom there were 8 images taken over the 360-degree rotation, yielding one image taken every 45 degrees. With IsoCal the BBs move a lot less between images because of the small rotation angle between them. This makes automatic tracking of the BBs much more efficient and easier with the IsoCal system. With the custom phantom the BBs move quite a bit between images and can make tracking the BBs more difficult, especially when the couch is angled, and makes it almost impossible for an automatic program to track multiple BBs moving large distances between images. The low number of images also creates issues with error.

As described before, the error calculated with the custom phantom was higher than the error produced in the TrueBeam tests with Clivio et. al. The low number of images used in the custom phantom are certainly an area of increased error. With lower images comes a higher overall error when correlating all the BBs paths. In theory, this is further exaggerated when the BB is moved farther away from the rotation axis. When the BB is moved farther away from the rotation axis, as seen in the Clinac iX experiment with the intentional 2 cm offset, the BB will travel an even greater distance between images, increasing the overall error between user selection points. This would likely be alleviated with taken more images, maybe at 20-degree intervals, or 10-degree intervals. Unfortunately, this angle difference between images is a limitation of the older linacs hardware and software. While the newer linacs have the programming to take images as the gantry continuously moves, the older linacs must be stationary when taking megavolt (MV) images, greatly increasing the time it takes to gather all the images. This process puts the image gathering for the experiment of the custom phantom on par with the time and method it takes to conduct a Winston-Lutz test.

Chapter 5. Conclusions

Overall, the custom phantom and the MATLAB program developed for this study produce comparable data to that produced by Varian's IsoCal and the Winston-Lutz test. The data achieved by this study was within a tenth of a millimeter of the IsoCal results from both the Emory University Hospital's TrueBeam and the TrueBeam used in the Clivio et. al. verification. One noticeable difference between the Varian IsoCal results and the results in the phantom is the error associated with the isocenter calculations. With the custom phantom, the isocenter calculations averaged around 0.525mm, which is just above the 0.5mm threshold for clinical isocenter verification. While this result is not ideal, it does prove that the image gathering is adequate, and the image processing does remain sub-millimeter and close to Varian's IsoCal verification method. With further work the process and code can be improved to likely get isocenter calculations within the 0.5 mm tolerance using the custom phantom. Creating an automatic tracking system in the program could also help with determining the results faster and more accurately than Winston-Lutz tests using radiographic film. Breaking down each component of the experiment yields strong points to feasibility and some short comings that would need to be tweaked.

Appendix A – The MATLAB Program

```
% UI to ask user if the DICOM image have been loaded
button = questdlg(sprintf('Have the .dcm files been loaded into MATLAB?\nIf unsure,...
       press "No".'),'Loading .dcm File','Yes','No','No');

% String comparison determined what user selected.
TF1 = strcmp(button,'No');

% Second UI that asks whether the BB locations have already been selected
if TF1 == 0
    button2 = questdlg(sprintf('Have the BB locations in all the images been...
              selected?\nIf unsure, press "No".'),'BB Selection','Yes','No','No');
    TF2 = strcmp(button2,'No');
else
    TF2 = 0;
    clear all
    close all
    TF1 = 1;
end

% If user selected 'No' then If statement runs to allows data loading.
if TF1 == 1


% Original working directory path (print working directory)
    Opath = pwd;

% Filter spec
    filter = {'.dcm'};

% "file" contains the file name, "path" contains the directory of the file.
    [file,path] = uigetfile(filter,'Select File','Multiselect','on');

% Changes the working directory of the MATLAB to that of where the file is
%contained.
    cd(path)

    numfiles = size(file,2);

% For loop to load the files into a readable cell array
    for i =1:numfiles

        info{i} = dicominfo(cell2mat(file(1,i)));


        Pic{i} = dicomread(cell2mat(file(1,i)));

    end
% range value set for BB selection range
    range = 15;

% Directory change to MATLAB files folder for function to work
    cd('C:\Users\MATLAB Files')

end

% If statement that allows BB selection to occur
if TF1 == 1 || TF2 == 1

% Main for loop that processes BB selection points from user and calculates
```

```matlab
%   BB tracking data
    for i = 1:numfiles
        figure (1)
        imshow(Pic{1,i},[])

        % For loop used for BB selection in figures
        for j = 1:12

            % UI selection and plot overlay
            title(['Image: ' num2str(i) '/' num2str(numfiles) ', BB: ' num2str(j)...
                    '/12'])
            [hx(i,j), hy(i,j)] = ginput(1);
            hx(i,j) = round(hx(i,j)); % Column value is rounded to whole number
            hy(i,j) = round(hy(i,j)); % Row value is rounded to whole number
            hold on
            plot([hx(i,j)-range hx(i,j)+range hx(i,j)+range hx(i,j)-range hx(i,j)...
                    range],[hy(i,j)-range hy(i,j)-range hy(i,j)+range hy(i,j)+range...
                    hy(i,j)-range],'g','markersize',15,'LineWidth',1.5)

            % BB center calculation function that passes values from UI
            %   selection
            [MeanCol80(i,j), MeanRow80(i,j), MeanCol50(i,j), MeanRow50(i,j),...
                    StdRow50(i,j),StdRow80(i,j), StdCol50(i,j), StdCol80(i,j)]...
                    = BBcenterFunct(Pic{1,i}, hx(i,j), hy(i,j));



% BB Center Calculation Function ***************************************************
function [MeanCol80, MeanRow80, MeanCol50, MeanRow50, StdRow50, StdRow80, StdCol50,...
       StdCol80]=BBcenterFunct(Pic, hx1, hy1)

range = 15;

% Determines high pixel and low pixel value in user selection range
HighPix = max(max(Pic(hy1-range:hy1+range,hx1-range:hx1+range)));
LowPix = min(min(Pic(hy1-range:hy1+range,hx1-range:hx1+range)));

% Creates empty matrices for value entry
Square80 = [];
Row80 = [];
Col80 = [];

Square50 = [];
Row50 = [];
Col50 = [];

% Main for loop that determines if values lie within range and are part of
%   BB pixels
for i = hx1-range:hx1+range
    for j = hy1-range:hy1+range

        % Determines if pixel values are above 80% attenuation range and
        %   put it in matrix, or puts in 0 if cell value fails
        if Pic(j,i) >= (HighPix-(ceil((HighPix-LowPix)*.2)))
            Square80(i,j) = Pic(j,i);
            Row80 = [Row80,j];
            Col80 = [Col80,i];
        else
            Square80(i,j) = 0;
        end

        % Determines if pixel values are above 50% attenuation range and
        %   put it in matrix, or puts in 0 if cell value fails
```

```
        if Pic(j,i) >= (HighPix-(ceil((HighPix-LowPix)*.5)))
            Square50(i,j) = Pic(j,i);
            Row50 = [Row50,j];
            Col50 = [Col50,i];
        else
            Square50(i,j) = 0;
        end
    end
end

% Uses mean value to determine center of pixels that qualify and determines
%   standard deviation of center
MeanRow80 = mean(Row80);
StdRow80 = std(Row80);
MeanCol80 = mean(Col80);
StdCol80 = std(Col80);

MeanRow50 = mean(Row50);
StdRow50 = std(Row50);
MeanCol50 = mean(Col50);
StdCol50 = std(Col50);
end
% End of BB Center Function ******************************************************


        end
    end
end

% For loop that organizes data based on zero degree couch angle or specified
%   couch angle
for m = 1:12

    BBloc50Straight(m,:) = [mean(MeanCol50(1:(numfiles/2),m)),...
             mean(MeanRow50(1:(numfiles/2),m))];
    BBloc80Straight(m,:) = [mean(MeanCol80(1:(numfiles/2),m)),...
             mean(MeanRow80(1:(numfiles/2),m))];

    BBloc50Angle(m,:) = [mean(MeanCol50((numfiles/2)+1:numfiles,m)),...
        mean(MeanRow50((numfiles/2)+1:numfiles,m))];
    BBloc80Angle(m,:) = [mean(MeanCol80((numfiles/2)+1:numfiles,m)),...
        mean(MeanRow80((numfiles/2)+1:numfiles,m))];

    StdDev50Straight(m,:) = [std(StdCol50(1:(numfiles/2),m)),...
             std(StdRow50(1:(numfiles/2),m))];
    StdDev80Straight(m,:) = [std(StdCol80(1:(numfiles/2),m)),...
             std(StdRow80(1:(numfiles/2),m))];

    StdDev50Angle(m,:) = [std(StdCol50((numfiles/2)+1:numfiles,m)),...
        std(StdRow50((numfiles/2)+1:numfiles,m))];
    StdDev80Angle(m,:) = [std(StdCol80((numfiles/2)+1:numfiles,m)),...
        std(StdRow80((numfiles/2)+1:numfiles,m))];
end
```

Appendix B – The Experimental BB Data

B.1 Varian Trilogy BB data using 50% penumbra value

BB Number	Couch Angle (Degrees)	Average BB location (x_{rot}, y_{rot})	$(\sigma_{x_{rot}}, \sigma_{y_{rot}})$
1	0	(510.458, 269.241)	(1.024, 1.901)
	20	(510.936, 295.308)	(1.524, 1.521)
2	0	(510.609, 300.026)	(0.726, 1.876)
	20	(510.523, 343.203)	(1.283, 1.971)
3	0	(511.163, 324.759)	(0.878, 1.834)
	20	(510.641, 270.997)	(1.133, 1.601)
4	0	(511.333, 345.369)	(1.085, 2.133)
	20	(510.910, 383.263)	(1.137, 2.229)
5	0	(510.906, 375.862)	(0.757, 1.329)
	20	(511.040, 399.799)	(0.886, 1.444)
6	0	(510.478, 402.578)	(1.180, 2.005)
	20	(510.647, 342.149)	(1.055, 1.724)
7	0	(510.471, 422.914)	(1.121, 1.992)
	20	(510.279, 468.579)	(0.937, 2.020)
8	0	(510.729, 452.430)	(0.912, 1.969)
	20	(510.833, 454.479)	(1.259, 2.010)
9	0	(510.880, 479.494)	(0.276, 1.367)
	20	(510.811, 419.718)	(0.985, 1.972)
10	0	(511.035, 499.760)	(0.929, 1.416)
	20	(510.889, 549.603)	(1.073, 1.962)
11	0	(511.317, 529.009)	(1.462, 1.958)
	20	(510.930, 507.044)	(1.216, 2.000)
12	0	(510.889, 556.342)	(0.981, 1.957)
	20	(510.653, 502.196)	(1.133, 1.699)

B.2 Varian Clinac iX BB data using 50% penumbra value

BB Number	Couch Angle (Degrees)	Average BB location (x_{rot}, y_{rot})	$(\sigma_{x_{rot}}, \sigma_{y_{rot}})$
1	0	(511.996, 218.121)	(1.122, 1.924)
	15	(511.773, 193.849)	(1.008, 1.838)
2	0	(511.153, 245.007)	(1.391, 1.695)
	15	(511.593, 297.487)	(1.316, 2.011)

3	0	(511.201, 275.686)	(0.905, 1.845)
	15	(511.451, 266.358)	(0.806, 1.727)
4	0	(511.780, 294.165)	(1.401, 2.242)
	15	(511.962, 279.767)	(1.522, 2.251)
5	0	(511.769, 321.967)	(0.913, 1.957)
	15	(511.789, 372.544)	(0.964, 1.938)
6	0	(512.337, 352.453)	(0.940, 2.005)
	15	(511.526, 328.235)	(1.128, 2.012)
7	0	(512.172, 371.654)	(1.034, 2.025)
	15	(511.590, 369.045)	(1.024, 2.095)
8	0	(511.596, 398.908)	(0.634, 1.395)
	15	(512.159, 443.138)	(0.609, 1.356)
9	0	(511.258, 429.784)	(0.948, 1.959)
	15	(511.192, 391.290)	(1.040, 2.108)
10	0	(511.926, 448.834)	(1.095, 1.859)
	15	(511.078, 458.444)	(0.954, 1.627)
11	0	(511.684, 475.288)	(0.670, 1.942)
	15	(511.912, 508.542)	(1.026, 2.002)
12	0	(511.777, 506.118)	(0.892, 1.782)
	15	(512.354, 458.899)	(1.334, 1.544)

B.3 Varian Clinac iX BB data with 2 cm offset using 50% penumbra value

BB Number	Couch Angle (Degrees)	Average BB location (x_{rot}, y_{rot})	$(\sigma_{x_{rot}}, \sigma_{y_{rot}})$
1	0	(512.148, 218.363)	(1.317, 2.007)
	15	(511.721, 213.174)	(1.023, 1.940)
2	0	(511.120, 244.936)	(1.384, 2.145)
	15	(511.275, 316.392)	(1.295, 2.004)
3	0	(511.278, 276.104)	(0.753, 1.737)
	15	(511.569, 285.304)	(0.818, 1.826)
4	0	(511.932, 294.689)	(1.367, 2.209)
	15	(511.990, 299.021)	(1.526, 2.248)
5	0	(512.040, 321.730)	(1.329, 1.968)
	15	(511.530, 391.714)	(1.337, 1.829)
6	0	(512.374, 352.928)	(1.034, 2.063)
	15	(511.505, 347.198)	(1.119, 1.970)
7	0	(512.000, 371.710)	(1.124, 2.051)
	15	(511.383, 388.160)	(0.845, 2.102)
8	0	(511.517, 399.061)	(0.443, 1.352)
	15	(511.802, 463.065)	(0.754, 1.583)
9	0	(511.715, 429.349)	(0.908, 1.935)

	15	(511.467, 410.267)	(0.988, 2.054)
10	0	(511.454, 449.552)	(1.009, 1.893)
	15	(510.727, 477.573)	(0.700, 1.525)
11	0	(511.677, 475.138)	(0.829, 1.912)
	15	(511.771, 527.604)	(1.059, 1.984)
12	0	(512.160, 505.671)	(0.826, 1.509)
	15	(511.894, 477.886)	(1.032, 1.323)

B.4 Varian TrueBeam BB data using 50% penumbra value

BB Number	Couch Angle (Degrees)	Average BB location (x_{rot}, y_{rot})	$(\sigma_{x_{rot}}, \sigma_{y_{rot}})$
1	0	(640.883, 436.375)	(0.831, 1.702)
	15	(640.732, 399.907)	(0.808, 1.222)
2	0	(640.035, 467.829)	(0.902, 1.592)
	15	(639.940, 462.406)	(0.814, 1.493)
3	0	(640.333, 506.959)	(0.821, 1.319)
	15	(640.378, 571.033)	(0.814, 1.502)
4	0	(640.726, 525.219)	(0.333, 1.037)
	15	(640.696, 473.558)	(0.474, 1.441)
5	0	(640.821, 557.960)	(0.805, 1.742)
	20	(641.008, 566.808)	(0.981, 1.720)
6	0	(641.304, 596.227)	(0.846, 1.697)
	15	(641.119, 647.239)	(0.990, 1.717)
7	0	(641.373, 614.471)	(0.946, 1.717)
	15	(641.145, 555.180)	(0.884, 1.509)
8	0	(640.750, 648.429)	(0.999, 1.560)
	15	(640.802, 673.503)	(1.018, 1.458)
9	0	(640.427, 685.594)	(0.751, 1.731)
	15	(640.819, 718.136)	(0.934, 1.654)
10	0	(640.586, 705.163)	(0.692, 1.474)
	15	(641.087, 640.840)	(1.068, 1.765)
11	0	(640.063, 737.996)	(0.934, 1.626)
	15	(640.465, 774.276)	(0.912, 1.686)
12	0	(641.140, 774.021)	(0.920, 1.358)
	15	(640.630, 786.913)	(0.780, 1.319)

References:

[1] Baker, Mitzi. "Medical linear accelerator celebrates 50 years of treating cancer." Stanford University. https://news.stanford.edu/news/2007/april18/med-accelerator-041807.html.

[2] Wiehle, Rolf, Hans-Jurgen Koth, Norbert Nanko, Anca-Ligia Grosu, and Norbert Hodapp. "On the Accuracy of Isocenter Verification with kV Imaging in Stereotactic Radiosurgery." *Radiotherapy and Oncology – Springer*, Vol. 185, Issue 5 (May 15, 2009): Pgs 325-30. MEDLINE – EBSCO.

[3] Lutz, Wendell, Ken Winston, and Nasser Maleki. "A System for Stereotactic Radiosurgery with a Linear Accelerator." *International Journal of Radiation Oncology, Biology, Physics*, Vol. 14 (February 1988): Pgs 373-81.

[4] "Imaging & Geometry Calibrations Overview." Varian Medical Systems. DCID: TB2.5-CEM-02-A

[5] Clivio, Alessandro, Eugenio Vanetti, Steven Rose, Giorgia Nicolini, Maria F. Belosi, Luca Cozzi, Christof Baltes, and Antonella Fogliata. "Evaluation of the Machine Performance Check application for TrueBeam Linac." *Radiation Oncology*, Vol. 10 (April 21, 2015): Pg 97. MEDLINE - EBSCO.

[6] Mao, Weihua, Louis Lee, and Lei Xing. "Development of a QA phantom and automated analysis tool for geometric quality assurance of on-board MV and kV x-ray imaging systems." *Medical Physics*, Vol. 34, Issue 4 (April 2008): Pgs 1497-506. MEDLINE - EBSCO.

[7] Sun B, SM Goddu, S Yaddanapudi, C Noel, and H Li. "Daily QA of linear accelerators using only EPID and OBI." *Medical Physics*, Vol. 42, Issue 10 (October 2015): Pgs 5584-94. MEDLINE - EBSCO.

[8] Rowshanfarzad, Pejman, Conor K. McGarry, Michael P. Barnes, Masheed Sabet, and Martin A. Ebert. "An EPID-based method for comprehensive verification of gantry, EPID and the MLC carriage positional accuracy in Varian linacs during arc treatments." *Radiation Oncology*, Vol. 9 (November 26, 2014): Pg 249. MEDLINE - EBSCO.